Reprinted from Preprint Volume: 21st Conference on Radar Meteorology, September 19-23, 1983, Edmonton, Alta., Canada. Published by the American Meteorological Society, Boston, Mass.

10.2

THREE-DIMENSIONAL WIND FIELD IN THE DEVELOPING INNER CORE OF HURRICANE DEBBY

Frank D. Marks, Jr.
Atlantic Oceanographic and Meteorological Laboratory
National Oceanic and Atmospheric Administration
Miami, Florida 33149

Robert A. Houze, Jr.
Department of Atmospheric Sciences
University of Washington
Seattle, Washington 98195

1. INTRODUCTION

Until recently detailed wind patterns in hurricane eyewalls and rainbands could be obtained only by constructing composites based on measurements made along aircraft flight tracks (Shea and Gray, 1973; Barnes et al., 1983; Jorgensen, 1983a,b). These composites have provided a good first approximation to eyewall and rainband circulations; however, they yield limited information on spatial and temporal variability. Generally, they show structures in two-dimensional, radial-height cross sections. With the advent of the NOAA airborne pulse-Doppler radar (Trotter et al., 1981; Jorgensen et al., 1983), it has become feasible to measure nearly simultaneously the horizontal wind field throughout a large three-dimensional volume of space surrounding the aircraft.

This technique is based on measurements of the mean Doppler radial velocity components of echoes detected with an X-band radar located in the tail of a National Oceanic and Atmospheric Administration WP-3D research aircraft. The antenna of this radar points normal to the fuselage and sweeps circularly through elevation angles of 0 to 360 deg.*

2. LARGE-SCALE STORM STRUCTURE AND FLIGHT PATTERN

During the period of our analysis (1950-2045 14 September 1982), Debby was located near 25 deg N, 69 deg W and was moving toward the north- northeast at 4-5 m/s. The storm was increasing in intensity (it actually did not reach hurricane status until 0000 GMT 15 September), and an eyewall was forming. While the aircraft was in the storm, the central surface pressure was 995 mb, and the peak wind speed encountered by the aircraft (flying at 450 m altitude) was 30-35 m/s.

*Other characteristics of the tail radar are given by Jorgensen (1983a).

Figure 1 shows a time-composite low-level reflectivity pattern detected by the WP-3D's lower fuselage radar. This radar is a C-band, 1.1 deg horizontal beamwidth radar, which scans horizontally. [See Houze et al. (1981) for other characteristics of this radar.] The flight track in Fig. 1 was obtained by plotting the aircraft position in a rectangular Cartesian grid whose origin [point (0,0) in Fig. 1] was always located at the center of the storm. The storm track was determined objectively using a procedure described by Willoughby and Chelmow (1982). The time-composite reflectivity pattern was constructed by mapping each ray of data collected with the lower fuselage radar into the rectangular grid attached to the storm center. When more than one reflectivity measurement was mapped into a particular grid square, the largest value was taken to be the best estimate of the reflectivity in that grid square. This procedure, used previously by Marks (1981), minimizes the effects of attenuation and beam geometry in producing underestimates of the reflectivity.

Figure 1 shows that a symmetric eyewall was not present during the time period under consideration. However, a prominent rainband curved around the north side of the storm. Peak reflectivities in this band were 40-44 dBZ near the end of the band, west-northwest of the storm center. Later in the day, a portion of this rainband wrapped around the center of the storm and took on the appearance of a mature eyewall. Hence, we refer to the strong curved rainband seen at the time of Fig. 1 as a "developing eyewall." An area of weak stratiform precipitation (with reflectivity below the lowest threshold shown in Fig. 1) existed to the west of the storm center, just outside the developing eyewall. A stratiform rainband was located still farther west, centered along the east-west coordinate -70 km. The highest reflectivities in this stratiform band were only 23-25 dBZ.

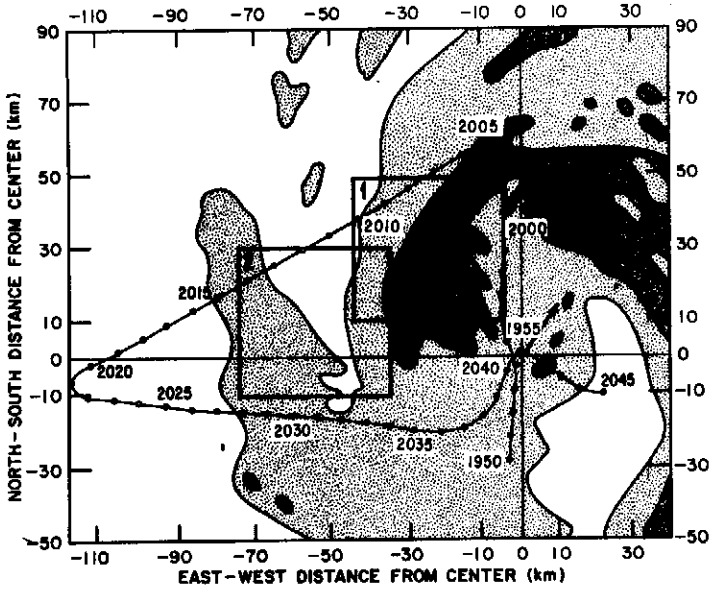

Figure 1. Time composite of the horizontal distribution of reflectivity in Hurricane Debby for 1950-2045 GMT 14 September. The reflectivity contours are for 20, 30 and 40 dBZ. The aircraft flight track is indicated by the thin solid line, and the three-dimensional analysis Boxes 1 and 2 are denoted by the thick solid lines. The origin of the coordinate system is located at the storm center, and the aircraft positions have been plotted in relation to the storm center.

3. METHOD OF ANALYSIS

The three-dimensional patterns of reflectivity, horizontal wind and divergence were determined from the tail radar for two analysis boxes, labelled 1 and 2 in Fig. 1. Each box was 40 km x 40 km in the horizontal and 15 km in vertical extent. Box 1 was chosen to cover an intense portion of the developing eyewall, while Box 2 enclosed the area of lighter precipitation just outside the developing eyewall and a portion of the weak stratiform rainband in the western part of the echo pattern in Fig. 1.

The reflectivity and wind analyses for Box 1 were constructed using the tail radar data obtained on the north-south flight leg from 1955-2004 GMT and the northeast-southwest leg from 2005-2014 GMT (Fig. 1). Analyses for Box 2 were constructed using the tail-radar obtained on the northeast-southwest flight leg from 2005-2014 GMT and the east-west leg from 2028-2035 GMT.

Three-dimensional time-composite reflectivity patterns were constructed for each box by a method analogous to that used to obtain the two-dimensional time-composite reflectivity map in Fig. 1. Each box was subdivided into grid elements 1 km x 1 km in the horizontal and 0.5 km in vertical dimension. Each ray of reflectivity data obtained with the tail radar, while flying along the flight legs contributing to each box, was mapped into the three-dimensional Cartesian grid contained in the box. Each datum taken from a ray was positioned at the center of the grid element into which it was mapped. When more than one reflectivity measurement was mapped into a particular grid element, the largest value was taken to be the best estimate of the reflectivity in that element.

Three dimensional fields of horizontal wind were constructed from the rays of radial velocity data obtained with the tail radar while the aircraft was flying along the two flight legs contributing to each analysis box. First, the radial velocities in each ray were examined and accepted only if the reflectivity was above a specified noise level (typically 6-10 dBZ). Then the accepted radial velocities in each ray were unfolded automatically using the method of Bargen and Brown (1980). The unfolded radial velocities were converted trigonometrically to horizontal wind components normal to the fuselage of the aircraft. The horizontal wind components thus obtained for one flight leg were then mapped into the three-dimensional Cartesian grid contained within the analysis box under consideration in the same manner as that used to map reflectivities into the three-dimensional grid. When more than one horizontal velocity component was mapped into a particular grid element, the average component was computed and used as the best estimate for that grid element. This procedure was repeated for the second flight leg contributing to the analysis box. Each grid volume then could contain averaged horizontal velocity components observed from 0, 1 or 2 viewing angles. For all grid volumes containing two components, the horizontal wind vector was computed. Thus, the three-dimensional field of horizontal wind was determined within Boxes 1 and 2. Further

details of this so-called "pseudo-dual Doppler" analysis method have been given by Jorgensen et al. (1983).

The fields of horizontal wind produced automatically by this method were inspected for spurious values generated by incorrect unfolding or other problems. The data were manually edited to remove these bad points.

The edited winds were smoothed by an overlapping filter applied at every grid point, with weightings of 0.125, 0.25, 0.5, 0.25 and 0.125 applied to adjacent points in both x and y. This process removes variability on scales less than 2 km in wavelength.

Three-dimensional fields of horizontal divergence were computed from the final edited and smoothed winds. The grid spacing in x and y used to compute the divergence was 2 km.

4. REFLECTIVITY AND WIND STRUCTURE IN BOX 1

The tail-radar reflectivity, wind and divergence analyses for Box 1 are shown in Fig. 2 for the 1, 3 and 5 km levels. These patterns depict the internal structure of the western portion of the developing eyewall rainband seen in Fig. 1. The reflectivity patterns in Fig. 2 show that at 1 km this region of the developing eyewall contained two sub-bands, an inner sub-band, intersecting the southern boundary of the box between -15 and -25 km, and an outer sub-band, intersecting the southern boundary between -30 and -40 km. The outer sub-band was generally more intense and extended upward through the 3 and 5 km levels. The inner sub-band sloped outward (from the storm center) and was very weak at 3 km and not apparent at 5 km, at which level it may have been merged with the outer sub-band.

In the wind patterns in Fig. 2, the wind speed can be seen generally to have decreased with increasing height, with zones of maximum speed at each height (enclosed by isotachs) corresponding closely to the sub-bands seen in the reflectivity data. At 1 km, the zone of peak wind speeds coincided with the inner sub-band. At 3 km, the southern core of maximum wind corresponded to the inner sub-band, while the northern wind maximum lay along the outer sub-band, just inside the axis of maximum reflectivity. At 5 km, a belt of maximum wind extended along the entire length of the outer sub-band of reflectivity.

Previous two-dimensional analyses based on flight-level wind data in hurricanes (Shea and Gray, 1973; Barnes et al., 1983; Jorgensen 1983a,b) have shown that wind speed maxima tend to occur within or just inside eyewalls and rainbands. Jorgensen's (1983a,b) studies indicate that the tangential wind maxium tends to lie inside the reflectivity maximum at low levels and coincide with it at about the 5 km level. If the outer sub-band in Box 1 is taken to be the major reflectivity feature, since it is stronger, has greater length and exhibits vertical continuity through all three levels in Fig. 2, then the wind maxima in our three-dimensional analysis exhibit the behavior expected from previous two-dimensional studies by lying well inside the outer sub-band at 1 km, and thence sloping upward to concide with the major sub-band at 5 km.

The divergence patterns derived from the winds at 1, 3 and 5 km are also shown in Fig. 2. These patterns were characterized by a curved band of convergence paralleling the sub-bands in the reflectivity field. At 1 km, the convergence band lay between the inner and outer sub-bands. At 3 km, the convergence band was more intense. Its axis lay a few kilometers to the inside of the line of maximum cores in the outer sub-band of reflectivity. At 5 km, the convergence band was as intense but not quite as widespread as at 3 km. The axis of the convergence band at 5 km coincided with the outer sub-band of reflectivity.

The two-dimensional analyses of Jorgensen (1983b) and Barnes et al. (1983) constructed from flight-level data indicate that the convergence zones associated with eyewalls and rainbands tend to slope radially outward with increasing height. Jorgensen's (1983b) study indicates that the eyewall convergence lies radially inside the maximum reflectivity at low levels and coincides with it at about the 5 km level. If the outer sub-band is considered to be the major feature in Box 1, then, again, the structure anticipated from these previous two-dimensional studies is seen in our data.

5. REFLECTIVITY AND WIND STRUCTURE IN BOX 2

It has long been recognized that hurricanes have extensive regions of stratiform precipitation (e.g., Atlas et al., 1963; Black et al., 1972; Hawkins and Imbembo, 1976). Jorgensen (1983a,b) has shown that stratiform precipitation is typically found in the region

Figure 2. Horizontal distribution of reflectivity (dBZ), wind (m/s) and divergence ($10^{-4}s^{-1}$) at 1 (bottom), 3 (middle) and 5 km (top) for Box 1. The east-west and north-south distances are in km from the storm center. The reflectivity is contoured at 0, 20, 30 and 40 dBZ. Streamlines (dark lines with arrowheads) and isotachs are shown in the wind analyses. At 1 km the isotach shown is for 31 m/s, at 3 km the isotach is for 24 m/s and at 5 km the isotach is for 14 m/s. The wind barb convention is: a flag represents 25 m/s; a full barb 5 m/s; and a half barb 2.5 m/s. Regions where divergence or wind estimates could not be obtained were left blank. The aircraft flight track is denoted on the wind maps as a thin continuous line with small arrowheads pointing in the direction of the flight.

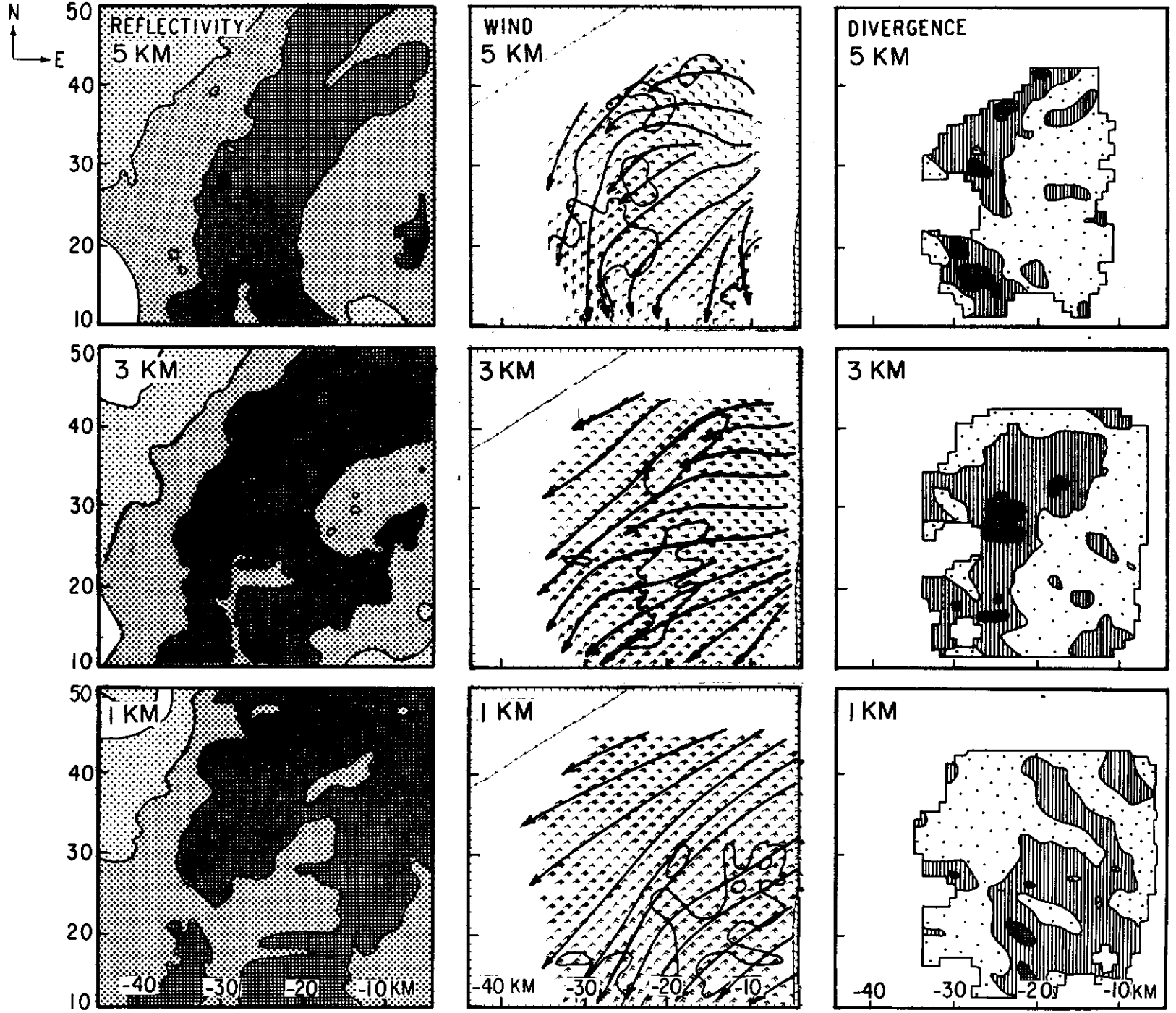
N
E
REFLECTIVITY
5 KM
WIND
5 KM
DIVERGENCE
5 KM
3 KM
3 KM
3 KM
1 KM
1 KM
1 KM
50
40
30
20
10
-40
-30
-20
-10 KM
-40 KM
-30
-20
-10
-40
-30
-20
-10 KM

just outside the eyewalls of mature hurricanes. Atlas et al. (1963) and Barnes et al. (1983) have found rainbands tending to be convective on their upwind ends and stratiform on their downwind ends. The existence of extensive stratiform precipitation in the vicinity of deep convection is also characteristic of tropical cloud clusters (Houze and Betts, 1981; Houze and Hobbs, 1982).

Box 2 (Fig. 1) was chosen for detailed analysis because it encloses a region of stratiform precipitation just outside the developing eyewall. This stratiform precipitation was found both in the weak rainband occupying the western part of Box 2 and throughout the intervening region of light rain between the weak rainband and the developing eyewall. The tail-radar analyses of the reflectivity, wind and divergence at the 1, 3 and 5 km levels in Box 2 are shown in Fig. 3. The patterns of these quantities in this stratiform region contrast sharply to the patterns in the more convective, developing eyewall region seen in Box 1 (Fig. 2).

The reflectivity patterns in Fig. 3 show the edge of the developing eyewall along the eastern side of Box 2, a region of weak stratiform echo in the center of the box and somewhat higher reflectivity on the western boundary, toward the center of the weak stratiform rainband.

The winds in this stratiform region are considerably more uniform in both speed and direction than in the developing eyewall region. Table 1 compares the means and standard deviations of the tangential and radial components of the wind (in a cylindrical coordinate system originating at the storm center) in Boxes 1 and 2. The standard deviations, particularly of the tangential component, are significantly lower in Box 2, the stratiform region. The magnitude of the divergence shown in Fig. 3 is also generally low throughout the stratiform region. In contrast to Box 1, no values exceeding 3 x 10^{-3} s^{-1} occurred for either divergence or convergence at any of the levels shown in Fig. 3.

In studies of the wind fields in the stratiform regions of tropical cloud clusters, Gamache and Houze (1982), Johnson (1982), and Houze and Rappaport (1983) have shown that a mesoscale downdraft and horizontal divergence predominate in the lower troposphere, while in the vicinity of and just above the melting level, mesoscale convergence predominates. The wind and divergence patterns in the western part of Box 2, occupied by the weak stratiform rainband, are consistent with this previously observed structure. At 5 km (about the top of the melting layer), the winds in the southwestern portion of Box 2 are generally confluent (except in the corner of the box) and convergence is indicated over this part of the box. At 3 km, diffluence and divergence are

Table 1. Mean and standard deviation of tangential and radial wind for Boxes 1 and 2.

Box 1

Altitude (km)	Tan. wind (s.d.) m s^{-1}	Rad. wind (s.d.)
1	26.6 (3.6)	-1.7 (4.5)
3	17.2 (3.1)	3.3 (3.4)
5	10.5 (3.2)	-1.7 (3.6)

Box 2

Altitude (km)	Tan. wind (s.d.) m s^{-1}	Rad. wind (s.d.)
1	16.0 (1.4)	5.6 (2.3)
3	15.0 (0.6)	-1.4 (2.2)
5	12.0 (0.6)	-7.2 (1.7)

indicated over the western part of Box 2. This change from mesoscale convergence to divergence downward across the melting layer is consistent with the structure of the stratiform regions of cloud clusters and suggests that a mesoscale downdraft may have been present in the mid-low troposphere of the stratiform rainband in the western part of Box 2. If present, however, the downdraft evidently did not penetrate into the boundary layer, since confluence and convergence occupied the western part of Box 2 at the 1 km level.

6. CONCLUSIONS

Analyses of data obtained with the X-band tail Doppler radar aboard a NOAA WP-3D research aircraft have provided three-dimensional patterns of reflectivity, wind and divergence in two contrasting regions of a storm developing to hurricane intensity. One region examined was the developing eyewall, while the other was a region of stratiform precipitation lying outside the developing eyewall. The three-dimensional patterns in these regions were consistent with structures anticipated from previous two-dimensional analyses of flight-level data obtained in hurricane eyewalls and rainbands, and from studies of wind data obtained in tropical cloud clusters.

In the developing eyewall region, the zones of maximum wind speed and convergence sloped radially outward from positions radially inside the primary sub-band of reflectivity in the developing eyewall at low levels to a position coincident with the primary sub-band at 5 km altitude. The detailed radar pattern showed further that the maximum wind at low levels was associated with a secondary sub-band, weaker and closer to the center of the storm than the primary sub-band. The consistency of the structure observed in the developing eyewall with eyewalls seen in previous studies of mature

Figure 3. Same as Fig. 2 for Box 2.

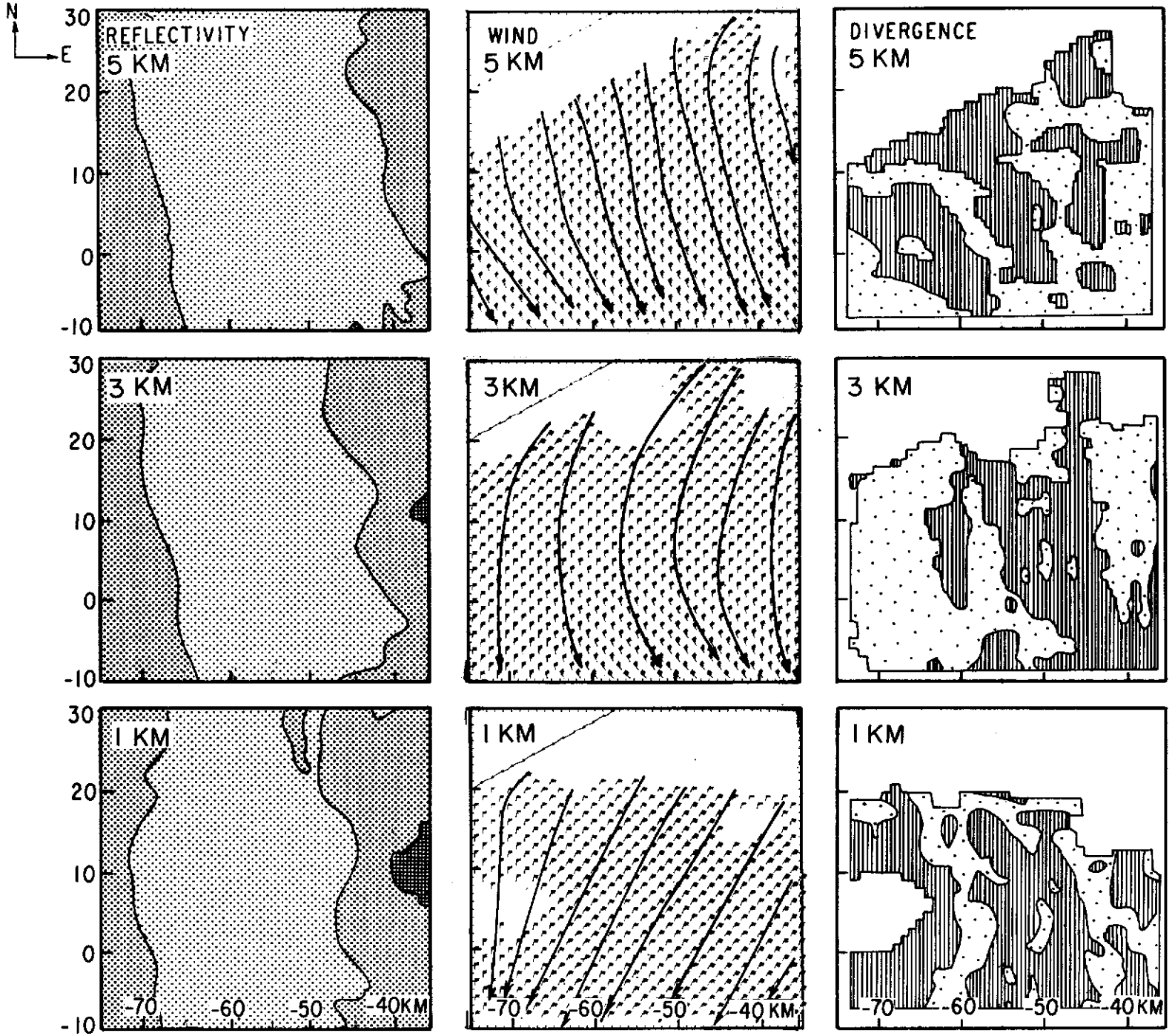
N
E
30
20
10
0
-10
REFLECTIVITY
5 KM
WIND
5 KM
DIVERGENCE
5 KM
3 KM
3KM
3 KM
1 KM
1 KM
1 KM
-70
-60
-50
-40KM
-70
-60
-50
-40 KM
-70
-60
-50
-40 KM

storms indicates that aspects of mature eyewall structure may already be present in storms still in the process of developing to hurricane intensity.

In the stratiform precipitation region, the winds were more uniform, and the intense zones of convergence seen in the developing eyewall region were absent. However, a broad region of confluence and convergence was seen at 5 km height, just above the melting layer, with diffluence and divergence covering the same broad region at 3 km. This change in sign of the divergence across the melting layer suggests that a mesoscale downdraft similar to those in the stratiform precipitation regions of tropical cloud clusters may have been present in this hurricane stratiform precipitation area.

The ability of the airborne Doppler radar to portray three-dimensional fields of the wind over large regions of a hurricane makes possible a wide range of future studies. We plan to continue to use the airborne Doppler system to examine the reflectivity and wind fields in eyewall and stratiform regions of mature and developing hurricanes to obtain a better understanding of their mass, momentum and water budgets.

8. ACKNOWLEDGMENTS

The data used in this study could not have been gathered without the aid of the NOAA Research Facilities Center flight crews and engineers, particularly Jim DuGranrut and Terry Schricker, who kept the airborne Doppler radar functioning during the 1982 hurricane season. Dave Jorgensen assisted in the design of the Doppler analysis software. One of the authors (RAH) was supported by the National Science Foundation under Grant No. ATM 80-17327.

REFERENCES

Atlas, D., K. R. Hardy, R. Wexler and R.J. Boucher, 1963: On the origin of hurricane spiral bands. Geofis. Int., 3, 123-132.

Bargen, D. W., and R. C. Brown, 1980: Interactive radar velocity unfolding. Preprints, 19th Conf. Radar Meteor., Amer. Meteor. Soc., Boston, 287-285.

Barnes, G. M., E. J. Zipser, D. Jorgensen and F. Marks, 1983: Interactions between convective vertical motions and mesoscale airflow through a hurricane rainband. J. Atmos. Sci. Accepted for publication.

Black, P. G., H. V. Senn, and C. L. Courtright, 1972: Airborne radar observations of eye configuration changes, bright band distribution and precipitation tilt during the 1969 multiple seeding experiments in Hurricane Debbie. Mon. Wea. Rev., 100, 208-217.

Gamache, J. F., and R. A. Houze, Jr., 1982: Mesoscale air motions associated with a tropical squall line. Mon. Wea. Rev., 110, 118-135.

Hawkins, H. F., and S. M. Imbembo, 1976: The structure of a small, intense hurricane-Inez 1966. Mon. Wea. Rev., 104, 418-442.

Houze, R. A., Jr., and A. K. Betts, 1981: Convection in GATE. Rev. Geophys. Space Phys., 16, 541-576.

Houze, R. A., Jr., and P. V. Hobbs, 1982: Organization and structure of precipitating cloud systems. Advances in Geophysics, 24, 225-315.

Houze, R. A., Jr., and E. N. Rappaport, 1983: Air motions and precipitating structure of an early summer squall line over the eastern tropical Atlantic. Submitted to J. Atmos. Sci.

Houze, R. A., Jr., S. G. Geotis, F. D. Marks, Jr., D. D. Churchill and P. H. Herzegh, 1981: Comparison of airborne and land-based radar measurements of precipitation during winter MONEX. J. Appl. Meteor., 20, 772-783.

Johnson, R. H., 1982: Vertical motion of near-equatorial winter monsoon convection. J. Meteor. Soc. Japan, 60, 682-690.

Jorgensen, D. P., 1983a: Mesoscale and convective-scale characteristics of mature hurricanes. Part I: General observations by research aircraft. Submitted to J. Atmos. Sci.

Jorgensen, D. P., 1983b: Mesoscale and convective-scale characteristics of mature hurricanes. Part II. Inner core structure of Hurricane Allen (1980). Submitted to J. Atmos. Sci.

Jorgensen, D. P., P. H. Hildebrand, and C. L. Frush, 1983: Feasibility test of an airborne pulse-Doppler meteorological radar. J. Appl. Meteor., 22, in press.

Marks, F. D., 1981: Evolution of the structure of precipitating convection in Hurricane Allen. Preprints, 20th Conf. Radar Meteor., Amer. Meteor. Soc., Boston, 720-725.

Shea, D. J., and W. M. Gray, 1973: The hurricane's inner core region, symmetric and asymmetric structure. J. Atmos. Sci., 30, 1544-1564.

Trotter, B. L., R. G. Strauch, and C. L. Frush, 1981: Evaluation of a meteorological airborne pulse-Doppler radar. NOAA Tech. Memo ERL WMPO-45, Boulder, Colorado, 55 pp.

Willoughby, H., and M. Chelmow, 1982: Objective determination of hurricane tracks from aircraft observations. Mon. Wea. Rev., 110, 1298-1305.